Automated instrumentation for miniaturized displacement electrophoresis with on-column photometric detection

Miroslava Šťastná, Vladislav Kahle, Karel Šlais*

Institute of Analytical Chemistry, Academy of Sciences of Czech Republic, 611 42 Brno, Czech Republic

Abstract

This paper describes an automated equipment for capillary displacement electrophoresis (isotachophoresis). The equipment employs the advantages of a separation channel with a nonuniform cross-section. The system works in a closed mode, the analytes are determined as anions in the examined arrangement. The pH gradient is within the range 4.4–11.0, the total voltage over the separation channel is from 150 V to 900 V at a constant current of 20 μA or 10 μA, respectively. Cetyltrimethylammoniumbromide and either hydroxypropylcellulose or hydroxypropylmethylcellulose are used in the leading electrolyte to control the electroosmotic flow.

The reproducibility and the minimum detectable concentrations are determined and calibration curves are measured using a model mixture of pI markers and myoglobin as analytes and either low-molecular-mass ampholytic buffers or synthetic carrier ampholytes as spacers. Both Gaussian peaks and the square-wave zones were evaluated.

Keywords: Capillary electrophoresis; Automation; Myoglobin; Ampholytes

1. Introduction

In addition to the methods known as isotachophoresis (ITP) [1,2], displacement electrophoresis [3], or isoelectric focusing (IEF) [4,5], intermediate techniques have recently been suggested as capillary electrophoretic methods for the separation and focusing of ampholytes, especially proteins. The intermediate techniques are either called isotachophoresis with carrier polyampholytes, capillary isoelectric focusing with electrophoretic mobilization (see Refs. [6,7] for review), or isotachophoresis–electric focusing [8]. Despite the differences in the names of the methods, the separation compartment in the recent instrumentation is rather uniform; it is based on the use of long flexible separation capillary of uniform cross-section placed between the sampling device and the on-column optical detector [3,8–13].

The use of a separation channel with nonuniform cross-section was predicted to bring some advantages in electrofocusing: the total voltage over the separation compartment should be lower and/or the separation capacity should be increased compared to that obtained with a capillary with a uniform cross-section [14,15]. However, modification of the capillary shape needs some adjustments both in terminology and instrumentation.

Since the zones can move with varying linear velocity along a separation channel with nonuniform cross-section, it is obvious that we cannot speak

*Corresponding author.

about isotachophoresis in this part of the instrument. Of course, under constant current conditions, we will have constant volume displacement or constant volume velocity. Nevertheless, the originally introduced term "displacement electrophoresis" (DE) [16] seems to be best suited for all techniques discussed above and is also applicable for non-constant volume displacement.

Further, the use of a capillary with a nonuniform cross-section brings about a substantial reduction in the overall channel length in IEF [17], in ITP [14], as well as in transition electrofocusing techniques [15,18]. The use of flexible capillaries becomes rather limited. Thus, the short separation channel with nonuniform cross-section needs to be essentially rigid and has to be integrated with the sampling device and the detection cell. Concepts previously used for the construction of the separation channel in the organic glass [19,20] or on the glass chip [21,22] come into consideration.

The automated instrumentation suggested in this contribution for capillary displacement electrophoresis (CDE) integrates the previously described liquid handling device [23] and the on-column photometric detector employing optical fiber technology [24] with the separation channel of nonuniform cross-section. To examine the instrument performance, the low-molecular-mass colored ampholytes described previously [25,26] and myoglobin were used as model analytes.

2. Experimental

2.1. Instrument description

A schematic representation of the suggested instrument is presented in Fig. 1. The separation compartment consisted of three blocks (1, 5 and 7) manufactured from plastics. The blocks were connected by means of threads sealed by Teflon foil. Block (1) made from organic glass enabled visual observation of the colored sampled zones during sampling and focusing in tapered channel (3). This channel was bored with a special tool and its inner wall was not modified. The liquids entered the tapered separation channel through the fused-silica capillary (2) with a volume of 0.4 μl. The broader

inlet end of channel (3) was connected to the reservoir of the terminating electrolyte (12) by means of a connecting capillary in the side opening equipped with a membrane (10). Thus, the system could be considered as a closed system [12,13]. A platinum electrode (11) was placed in the reservoir of the terminating electrolyte (12).

The second block (5) was made from non-transparent polyvinyl chloride with cut-out windows. This block served to hold the fused-silica capillary (4) (53×0.25 mm I.D.; Lachema, Brno, Czech Republic), which was glued in both ends of the block (5). The inner surface of this fused-silica capillary was not modified. Optical transparency of the fused-silica capillary (4) was obtained by removal of the external polyimide layer in the flame of spirit burner. Two openings on the top of the block (5) served for the installation of the optical fibers for the inlet (6) and outlet (9) of the light to the detector.

The principle of the on-line fiber optical detection system used in our work was published earlier [24]. Compared with the referred article [24], important improvements were realized resulting in enhancement of the signal-to-noise ratio and in detector applicability. A LCD 2082 UV detector (ECOM, Prague, Czech Republic) working at variable wavelength was used. A spherical quartz lens with a diameter of 3 mm was used to focus the light into the optical fiber. The optical fibers (Polymicro Technologies, Phoenix, AZ, USA; type FVP) had a core diameter of 200 μm and the total length of 70 cm. They were transparent both in the visible and in the UV range of the spectrum. The ends of the fibers were glued into small stainless steel capillaries for easier manipulation and polished.

The third block (7), made from organic glass, served as a leading electrolyte reservoir. The capillary anode was fixed at the top of this block.

The electrodes were connected either to the laboratory-made power supply with an adjustable voltage limit up to 1 kV or to the Spellman (CZE 1000 R, New York, USA) power supply.

The whole separation compartment was fixed in the liquid distribution block (16) of the liquid handling instrument described previously [23]. The liquid distribution block included four liquid inlets (15) and an outlet to the fused-silica capillary (2) in block (1). Movement of the piston in the fixed
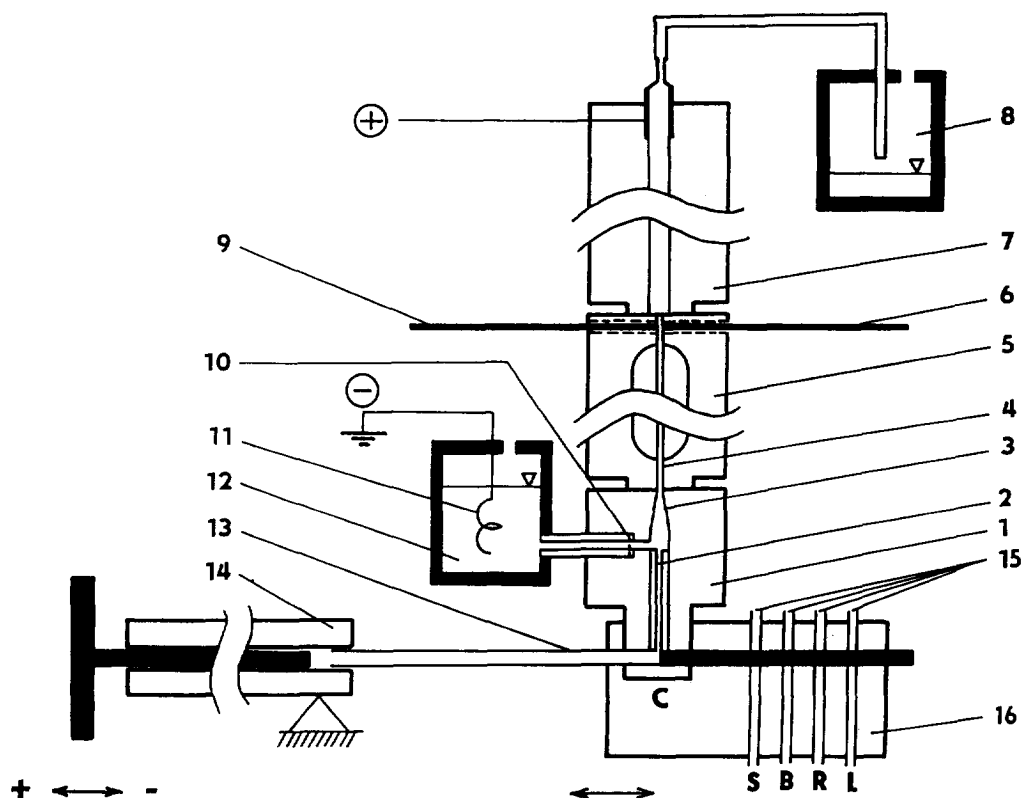
Fig. 1. Instrument design. (1) Plastic block, (2) fused-silica capillary of volume 0.4 μl (0.15 mm I.D.×23 mm; position C in Table 1), (3) tapered channel of volume 3 μl (the one end 0.8 mm I.D., the other end 0.4 mm I.D.×5 mm), (4) fused-silica capillary of volume 2.6 μl (0.25 mm I.D.×53 mm), (5) plastic holder, (6) optical fiber from the light source, (7) leading electrolyte reservoir of volume 120 μl, (8) waste, (9) optical fiber to the photodiode, (10) membrane with active area of 1 mm^2, (11) electrode, (12) reservoir of the terminating electrolyte of volume 2 ml, (13) injection needle (0.3 mm I.D.; 0.5 mm O.D.) with a side outlet (0.15 mm O.D.), (14) glass syringe of volume 100 μl, (15) inlets for sample (position S), background or spacers (position B), leading electrolyte (position L) and transport liquid (position R), (16) liquid distribution block.

glass-syringe with a volume of 100 μl (14) allowed suction and delivery of liquids and was driven by a step motor. The switching of liquids in the liquid distribution block was achieved by changing its position. Movement of block (16) was driven by a second step motor.

The whole procedure of rinsing with the leading electrolyte and injection of the sample, spacers and transport liquid into block (1) was controlled by a microprocessor programmed by the user according to desired analysis. After renewing of the electrolytes, the electrofocusing run was started by switching on the power supply adjusted to the desired constant current. A more detailed description of the instrument operation is given below.

A two-line recorder (TZ 4620, Laboratory Instruments, Prague, Czech Republic) was used to registrate the voltage and the detector signal.

2.2. Instrument function

The function of the apparatus is shown schematically in Fig. 2. The separation of anions was chosen. An example of the analysis program is given in Table 1.

The terminating electrolyte (T) was refreshed daily. The program for renewing the electrolytes included rinsing of the separation unit four times prior the analysis. The apparatus remained filled with leading electrolyte (L) after the last rinsing (Fig. 2A).
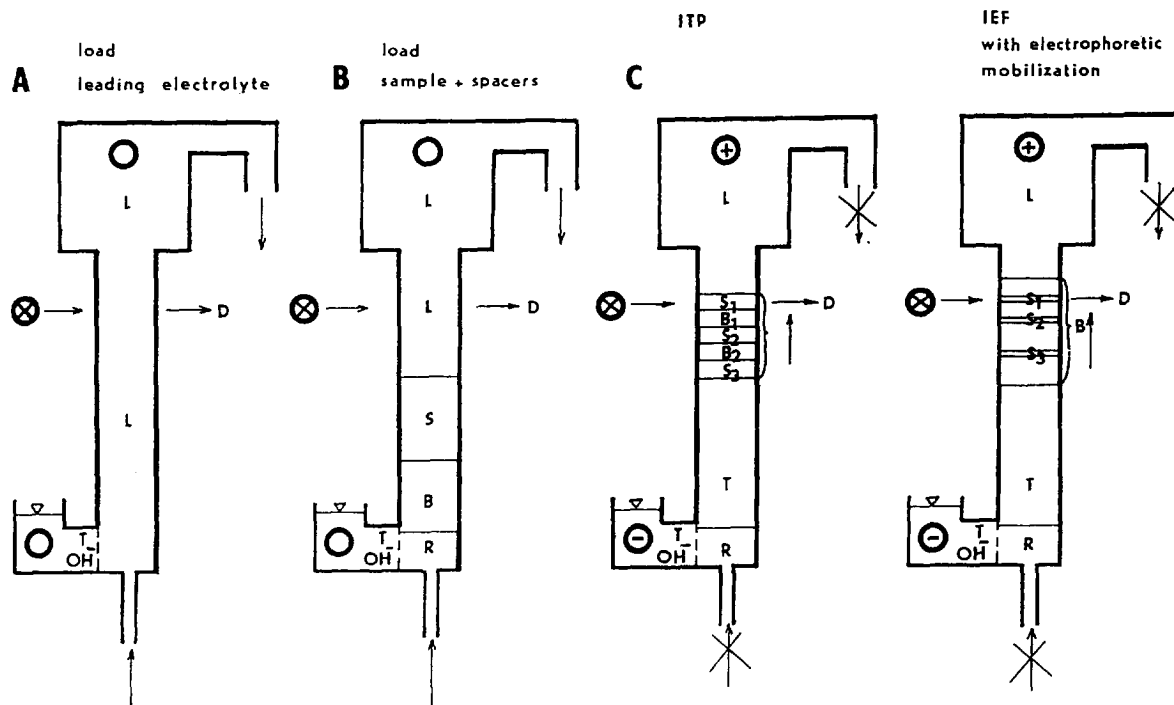
Fig. 2. Instrument function. (L) Leading electrolyte, (S) sample, (B) background or spacers, (R) transport liquid, (T) terminating electrolyte, (D) optical detector; for explanation see text.

Then, consecutively, 30 μl of the transport liquid (R), 0–1.5 μl of the solution of spacers (B1 to Bn) or Ampholine (B) and 0–1.5 μl of the sample solution (S1 to Sn) with a flow-rate of 10 μl min^{-1} were sucked into the syringe (14) and needle (13). Then, the needle volume and part of the content of

the syringe were transported to the separation compartment (Fig. 2B). The total volume injected into block (1) was up to 2 μl, which was the internal volume of the needle. The sample solution and spacer solution were always injected into the space above the upper end of the fused-silica capillary.

Table 1
Example of analysis program

Step no.	Needle position	Function	Volume (μl)	Flow-rate (μl min^{-1})	Voltage	Remarks
1	C	–	75	200	off	
2	L	+	75	200	off	Rinsing repetition
3	C	–	75	200	off	4× with L
10	R	+	30	200	off	
11	B	+	0.5	10	off	
12	S	+	1	10	off	
13	C	–	2	1	off	Injection S,B,R
14					ON	hydrodynamic flow stopped

C=inlet to the fused-silica capillary (2) in block (1); L=leading electrolyte; R=transport liquid; B=background or spacers; S=sample; +/− syringe function: suction/delivery

After injection of the sample and spacer solution into the space above the fused-silica capillary by means of the transport liquid (R), the hydrodynamic flow was stopped. Then, the power supply was switched on and the electrophoretic analysis ran under constant current conditions.

All ions moved to the corresponding electrodes, ions of the terminating electrolyte diffused through the membrane and analytes were separated gradually during their transport through the tapered channel and the coupled fused-silica detection capillary. Depending on the nature of the background and amount of analytes, the square-wave zones typical for ITP or Gaussian zones typical for IEF were obtained in the detector (Fig. 2C). When the voltage was switched on, the liquid did not flow in the apparatus.

2.3. Chemicals

All chemicals used were of analytical grade purity. Succinic acid, cetyltrimethylammoniumbromide (CTAB), glycerine, piperidine, $Ba(OH)_2$, KH_2PO_4, KOH and H_3PO_4 were obtained from Lachema (Brno, Czech Republic); 2-amino-2-methyl-1-propanol (AMP) and hydroxypropylmethylcellulose (HPMC) from Sigma (St. Louis, MO, USA) and hydroxypropylcellulose (HPC) from EGA Chemie (Steinheim/Albuch, Germany). 2-(N-Morpholino)-ethanesulphonic acid (MES) and N-(2-hydroxy-ethyl)piperazine-N'-(3-propanesulphonic acid) (HEPPS) were purchased from Merck (Darmstadt, Germany), L-histidine monohydrochloride (HIS) from Reanal (Budapest, Hungary) and L-lysin (LYS) from LOBA Chemie (Austria). The solution of synthetic carrier ampholyte Ampholine pH 3.5–10.0 was from Pharmacia LKB (Uppsala, Sweden). Horse heart myoglobin from Fluka AG (Switzerland, p*I* 6.8, M_r 17 800) was applied. The p*I* markers 6-nitro-2,4-bis(1-piperidinomethyl)phenol (**2**), 4-nitro-2,6-bis(N-methyl-1-piperazinomethyl)phenol (**3**), 4-nitro-2-(4-morpholinomethyl)phenol (**15**) and 2-chloro-6-nitro-4-(4-morpholinomethyl)phenol (**19**) were prepared in Institute of Analytical Chemistry (Academy of Sciences, Brno, Czech Republic). The numbers of p*I* markers are consistent with those mentioned in Refs. [25,27].

Table 2
List of mobility, pK_a and M_r of buffers[a]

Buffer	$u \times 10^9$ (m^2 V^{-1} s^{-1}]	pK_a'	pK_a''	M_r
Succinic acid (−1)	−35.2	4.21	5.64	118.1
(−2)	−57.2			
AMP	+29.5[b]	9.71		89.1
MES	−26.8	1.30	6.13	195.2
HEPPS	−20.9[c]	3.75	7.90	252.3
HIS	−28.3	6.13	9.33	155.2
LYS	−26.4	8.95	10.79	146.2

[a] Taken from Refs. [28–30].
[b] Estimated according to the mobility $+29.5 \cdot 10^{-9}$ m^2 V^{-1} s^{-1} of both Tris and 2-amino-2-methyl-1,3-propanediol (Amediol) [31].
[c] Determined by linear interpolation (see text).

2.4. Electrolyte systems

Table 2 includes a list of the analytes and their ionic mobility, u, logarithm of dissociation constant, pK_a, and relative molecular mass, M_r. The ionic mobility for HEPPS was determined from a graph of u vs. $1/\sqrt{M_r}$ constructed for similar substances with known ionic mobilities. Table 3 shows the p*I* markers and their pK_a values, isoelectric point, p*I*, M_r, their maximum absorption wavelength at the pH corresponding to their isoelectric point, $(\lambda_{max})_{pI}$, and the slope of the effective charge, z, versus pH at the isoelectric point, $(dz/dpH)_{pI}$. The pK_as for the p*I* markers indicate dissociation constants just below and above the isoelectric point of the corresponding p*I* marker.

A solution of succinic acid (leader) and AMP (counterion) was used as the leading electrolyte (L). The pH of the leading electrolyte was adjusted to pH 4.2–4.3 by changing the concentration of AMP. A solution of 0.01 mol l^{-1} $Ba(OH)_2$ and 0.1 mol l^{-1} piperidine (pH 12.2) was used as terminating electrolyte (T) in the initial analyses and a 0.01 mol l^{-1} AMP solution (pH 10.5) was used for most of the presented analyses.

CTAB and either HPC or HPMC were added to the leading electrolyte to modify the charge on the surface of the fused-silica detection capillary and to control electroosmosis.

A 10% (w/v) glycerine solution in distilled water was used as transport liquid (R). The spacer solution

Table 3
List of pK_a, pI, M_r, $\lambda_{max,pI}$ and $-(dz/dpH)_{pI}$ of pI markers[a]

Marker No.[b]	pK_a'	pK_a''	pI	M_r	$\lambda_{max,pI}$ (nm)	$-(dz/dpH)_{pI}$ (pH^{-1})
2	9.35[c]	10.90[c]	10.13	406.3	412	0.60
3	8.02[c]	9.27[c]	8.65	509.3	420	0.74
15	5.16	8.07	6.61	274.7	400	0.15
19	3.76	6.91	5.33	309.1	409	0.12

[a] Values taken from Refs. [25,26].
[b] Numbers correspond to Refs. [25,27].
[c] Values measured in this work by the method described earlier [25,26].

was a mixture of MES, HEPPS, HIS, LYS or a 1.4% (v/v) solution of synthetic carrier ampholyte Ampholine pH 3.5–10.0. The model analytes were pI markers and horse heart myoglobin. Titration curves of the pI markers are shown in Fig. 3 in the form of the charge (z) dependence on the pH. On the pH-axis, the pI values (effective charge $z=0$) for the individual markers are indicated.

To enable the photometric detection of both Gaussian and square-wave zones at the different pHs of the migrating zones, the spectral properties of the

Fig. 3. Titration curves of pI markers. (1) pI marker **19**, (2) pI marker **15**, (3) pI marker **3**, (4) pI marker **2**.

analytes were examined. The spectra obtained for the pI markers **19**, **15**, **3** and **2** (for numbers see Table 3 and Ref. [25]) are presented in Fig. 4. The pH values were chosen close to the isoelectric points of the analytes. The buffers used for this measurement were prepared from 0.1 mol l^{-1} KH_2PO_4 solution (pH 4.5) which was adjusted to the pH values needed with 1 mol l^{-1} KOH or 0.1 mol l^{-1} H_3PO_4 solution, respectively, and were mixed with solutions of the individual pI markers to give a final concentration allowing measurements within the range of absorbances of the applied instrument. The spectra were measured with a Varian 634 UV–Vis spectrophotometer (CA, USA) and the pH of the solutions was determined with a MS 22 pH meter (Laboratory Instruments, Prague, Czech Republic).

3. Results and discussion

3.1. Instrument design

As described in the preceding section, the CDE instrument was designed as a combination of the modified automated liquid handling instrument [23], the optic fiber UV detector [24] with the separation compartment consisting of the tapered organic-glass channel coupled with the fused-silica detection capillary (see Fig. 1). This system was employed for the following reasons: (1) There were satisfying experiences with the automated liquid handling instrument which enables handling of liquid volumes from few nanoliters up to milliliters against pressures up to tens of MPa [32,33]. (2) The vertical axis of the
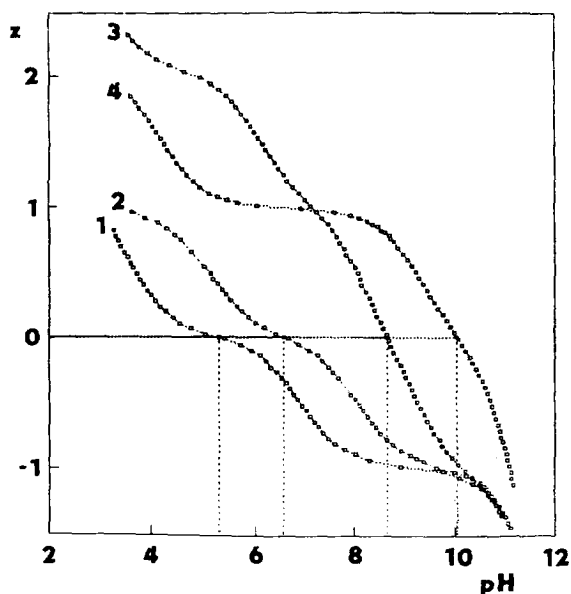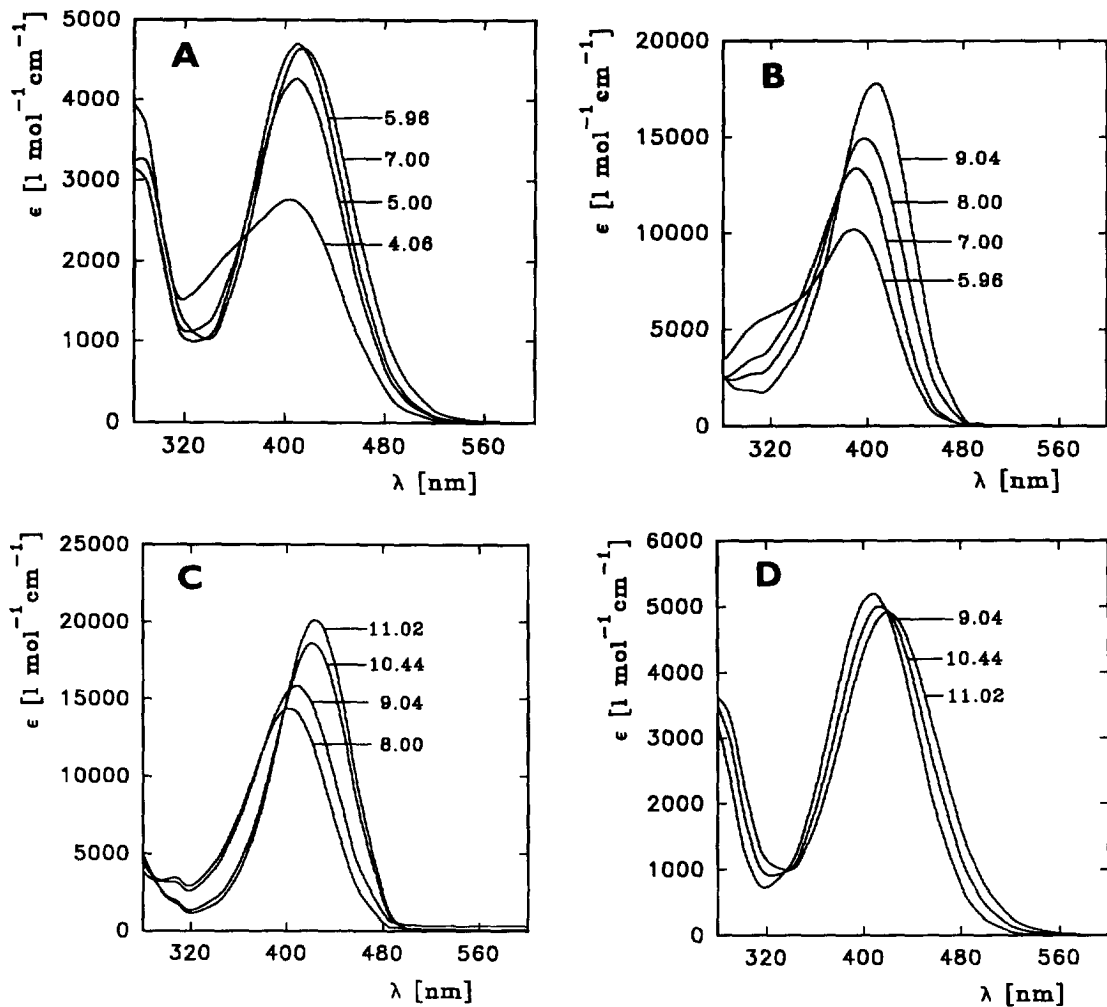
Fig. 4. Spectra of p*I* markers. [ε = Molar absorption coefficient (l mol⁻¹ cm⁻¹), λ = wavelength (nm)]. (A) Spectra of p*I* marker **19** for pH 4.06, 5.00, 5.96 and 7.00; (B) spectra of p*I* marker **15** for pH 5.96, 7.00, 8.00 and 9.04; (C) spectra of p*I* marker **3** for pH 8.00, 9.04, 10.44 and 11.02; (D) spectra of p*I* marker **2** for pH 9.04, 10.44 and 11.02.

separation compartment reduces problems with re-moval of bubbles. Additionally, since a possible thermal gradient [17] would produce a decrease in the liquid density in the upward direction this would not induce gravitational mixing. (3) The use of a closed system allows reproducible control of the migration time by the composition of the leading electrolyte. This is advantageous compared with ITP in open systems. Nevertheless, electroosmosis should be minimized. (4) The combination of the closed system and the high-pressure liquid handling instru-

ment removes the limitations imposed by the liquid viscosity on sampling. Flushing of the instrument functioned well even with a 66% sucrose solution with a viscosity of 180 mPa s (the viscosity of water is 1.00 mPa s at 20°C). According to the Poiseuille equation the pressure on the membrane (10) during rinsing with the 66% sucrose solution was calculated to be 0.39 MPa. (5) The use of the transport liquid (R) makes it possible to bring the sample into the proper position with respect to the terminating electrolyte (see Fig. 2B). Its density should be higher

than that of the other liquids to prevent mixing in the broader part of the tapered channel. Further, the conductivity of the transport liquid should be minimized to provide a high resistance of the liquid in the capillary (2) and electric insulation of the electrolyte system from the grounded liquid handling instrument. Thus, the voltage of the electrodes can be floating relative to the ground during the electrofocusing run. A possible decrease of the conductivity of the liquid in the broader part of the tapered channel does not cause a serious problem since the contribution of this part of the channel to the overall resistance is small due to the used geometry of the separation compartment. (6) In the tapered channel, the substances are separated and focused with a low total voltage drop over the separation compartment. In the arrangement used, the tapered channel made in the organic glass contributes to the volume of the separation compartment for 55%, while its contribution to the total resistance is only 3%. The organic glass is easy to machine, but its compatibility with UV detection is low. (7) In order to allow on-column UV detection, the outlet of the tapered channel was coupled to the fused-silica capillary (4). It was predicted that even a much shorter capillary with a constant cross-section should be sufficient to reach a steady-state zones [34]. In the fused-silica capillary (4) the focused zones move at constant velocity. Thus, the transparency and reasonable length of the fused-silica capillary (4) allow to observe the colored zones and to determine their absolute size and velocity. (8) The on-column optical fiber detection enables the flexible coupling of the detection cell with the detector optics which is needed in the used instrument design. The on-column detection cell with optical fibers can be regarded as the intersection of two cylinders. Since the actual diameters of the fiber core and the capillary internal diameter are comparable and the capillary wall acts like a cylindrical lens, the aperture can be approximated by the cross-section area of the fiber core. In accordance with Sternberg [35], the relationship for calculation of the standard deviation, σ_d, of the contribution of the circular aperture of diameter, d, to the zone broadening can be derived as $\sigma_d = d/\sqrt{20}$. For the diameter of the used fiber core (0.2 mm) σ_d equals 0.045 mm.

3.2. Characteristics of instrument performance

The electropherogram illustrating CDE of pI markers focused in the boundaries of between spacer zones is presented in Fig. 5. The peaks of pI markers **19, 15, 3** and **2** were separated by square-wave zones of MES, HEPPS, HIS and LYS. In order to eliminate the electroosmotic flow and to achieve sharp focused zones, CTAB with a final concentration of 0.1 mmol l^{-1} and HPC with a resulting concentration of 0.2% (w/v) were added to the leading electrolyte. The pI marker **19** was focused between the zones of MES and HEPPS, pI marker **15** between the zones of HEPPS and HIS, pI marker **3** between the zones of HIS and LYS, and pI marker **2** between the zones of LYS and terminating electrolyte as expected. The pH of the leading electrolyte was 4.3 and that of the
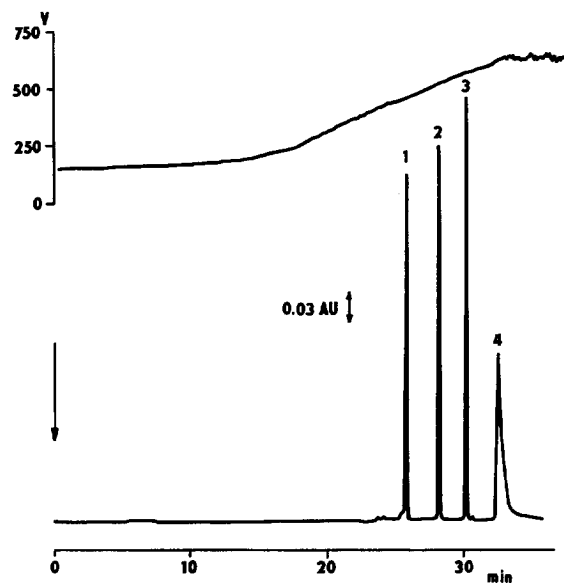

Fig. 5. CDE of pI markers focused in boundaries between discrete spacers. (1) pI marker **19** (65 μmol l^{-1}), (2) pI marker **15** (18 μmol l^{-1}), (3) pI marker **3** (13 μmol l^{-1}), (4) pI marker **2** (200 μmol l^{-1}). Conditions: leading electrolyte (pH 4.3), 25 mmol l^{-1} succinic acid and 19 mmol l^{-1} AMP, 0.1 mmol l^{-1} CTAB, 0.2% (w/v) HPC; terminating electrolyte (pH 12.2), 0.01 mol l^{-1} Ba(OH)$_2$ and 0.1 mol l^{-1} piperidine; spacers, MES (20 mmol l^{-1}), HEPPS (40 mmol l^{-1}), HIS (45 mmol l^{-1}), LYS (27 mmol l^{-1}); sample volume, 1000 nl; spacer volume, 300 nl; I=20 μA; λ=420 nm; home-made power supply.

terminating electrolyte was 12.2. The small peak at the beginning of the electropherogram determined the boundary between the leading electrolyte and the MES zone. Simultaneously with the detector output the voltage was registered during the analysis as shown in Fig. 5. The initial voltage was 150 V and it increased gradually to a final voltage of 650 V at a constant applied current of 20 μA.

To evaluate the instrument function, reproducibility and calibration curves were measured. Succinic acid (25 mmol l^{-1}) and 17 mmol l^{-1} AMP solution (pH 4.2) as the leading electrolyte and 10 mmol l^{-1} AMP (pH 10.5; 5 mmol l^{-1} AMP, respectively) as the terminating electrolyte were used for these measurements. The sample solution was prepared from a model mixture of the three p*I* markers **19, 15** and **3**; the spacer solution was a mixture of MES, HEPPS, HIS and LYS. The other conditions of analyses were the same as for the experiment illustrated in Fig. 5, except of the spacer solution which was three times diluted.

The relative standard deviations (R.S.D.) ($n=7$) were calculated as 1.1%, 3.4% and 5.5% for the peak area of p*I* markers **19, 15** and **3**, respectively, and as 3.8% and 3.2% for the lengths of the spacer zones of HEPPS and HIS measured as the distance between the peaks of the p*I* markers. When the 10 mmol l^{-1} AMP terminating electrolyte was replaced with 5 mmol l^{-1} AMP solution the results were similar.

Two kinds of calibration curves were measured for p*I* markers. First, the dependence of the peak areas on increasing injected sample volumes (from 0 to 1000 nl) with constant concentration (Table 4A) and second, the dependence of the peak areas on the concentration of the sample solution for a constant injected volume of 1000 nl (Table 4B). In the second case the sample solution was diluted 80-fold in four steps. The injected volume of spacer solution was 300 nl.

Calibration curves for spacers HEPPS and HIS were determined as the dependence of the lengths of the square-wave zones measured between the peaks of the p*I* markers on the injected volume of spacer solution (from 0 to 900 nl) with constant concentration. The volume of injected solution of p*I* markers was 600 nl. The results are given in Table 5.

Table 4 and Table 5 show the calculated values of

Table 4
Regression data of the calibration curves of p*I* markers

Marker No.	A			B		
	a	b	r	a	b	r
3	8	773	0.991	−86	5521	0.998
15	42	688	0.999	147	5833	0.999
19	15	1094	0.990	171	8469	1.000

(A) Variable injected volume at constant solution concentration; (B) variable solution concentration at constant injected volume; a and b are coefficients in the equation $y=a+bx$; $r=$correlation coefficient; $y=$peak area (mm^2); $x=$injected volume (nl) in A and solution concentration (mol l^{-1}) in B, respectively.

the correlation coefficient r, the intercept a and slope b in the linear equation ($n=3$).

In isotachophoresis, the peak shape of the detected substance between the zones of the individual spacers depends on its injected amount. We obtain the substance zone either as a Gaussian peak or as a square-wave form depending on the injection of either a small or a large amount. Square-wave forms are shown in Fig. 6, where the concentrations of the p*I* markers **19, 15** and **3** were approximately 37, 355 and 145 times higher than those in Fig. 5.

In the next analyses a 1.4% Ampholine solution was used instead of the mixture of individual spacers. The analysis of the model mixture of p*I* markers resulted in Gaussian peaks in the electropherogram. The minimum detectable concentrations of the p*I* markers were calculated and measured at such a sensitivity of the detector that the height of the noise of the base-line could be seen. The electropherogram is presented in Fig. 7. The concentrations of the p*I* markers **19, 15** and **3** in the sample solution were 10.6 μmol l^{-1}, 4.0 μmol l^{-1} and 2.8 μmol l^{-1}, respectively. The injected volume was 300 nl. The

Table 5
Regression data of the calibration curves of spacers

	a	b	r
HEPPS	2	52	0.989
HIS	3	45	0.994

a, $b=$coefficients in linear equation $y=a+bx$; $r=$correlation coefficient; $y=$square-wave zone length (mm); $x=$injected volume (nl).
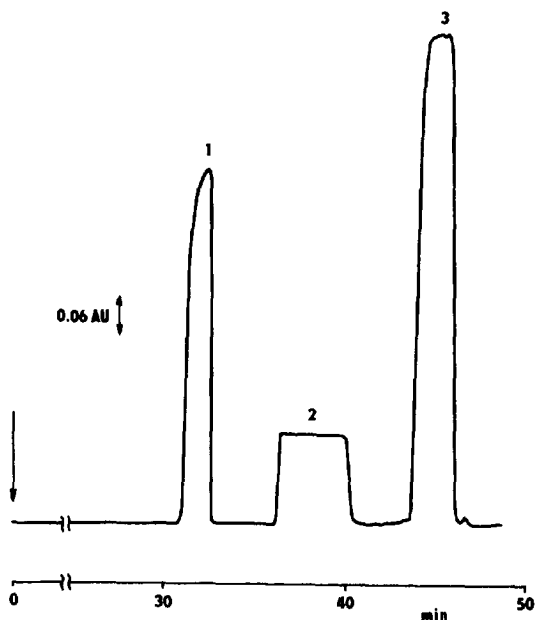
Fig. 6. CDE generating square-wave zones of pI markers and spacers. (1) pI marker 19 (2.4 mmol l^{-1}), (2) pI marker 15 (6.4 mmol l^{-1}), (3) pI marker 3 (1.9 mmol l^{-1}). Conditions: spacers, MES (18 mmol l^{-1}), HEPPS (45 mmol l^{-1}), HIS (41 mmol l^{-1}), LYS (25 mmol l^{-1}); leading electrolyte (pH 4.2), 25 mmol l^{-1} succinic acid and 17 mmol l^{-1} AMP, 0.1 mmol l^{-1} CTAB, 0.2% (w/v) HPC; terminating electrolyte (pH 12.2), 0.01 mol l^{-1} Ba(OH)$_2$ and 0.1 mol l^{-1} piperidine; sample volume, 1000 nl; spacer volume, 200 nl; I=20 μA; λ=478 nm; home-made power supply.

Fig. 7. CDE of trace amounts of pI markers in Ampholine background. (1) pI marker 19 (11 μmol l^{-1}), (2) pI marker 15 (4 μmol l^{-1}), (3) pI marker 3 (3 μmol l^{-1}). Conditions: leading electrolyte (pH 4.2), 25 mmol l^{-1} succinic acid and 17 mmol l^{-1} AMP, 0.15 mmol l^{-1} CTAB, 0.2% (w/v) HPC; terminating electrolyte (pH 10.5), 10 mmol l^{-1} AMP; background, 1.4% Ampholine pH 3.5–10.0; sample volume, 300 nl; background volume, 1000 nl; I=20 μA; λ=420 nm; Spellman power supply.

minimum detectable concentrations were determined as 1.6 μmol l^{-1}, 0.5 μmol l^{-1} and 0.7 μmol l^{-1}, respectively, for a signal-to-noise ratio of 2. To achieve optimal analytical conditions and sharp focused zones some parameters had to be optimized, e.g. the applied current and the concentration of CTAB in the leading electrolyte. When the current was increased from 20 μA to 24 μA or 30 μA faster analyses were obtained but the widths of the peaks increased at the same time. For lower current the analysis time increased considerably without substantial reduction of peak width. An optimal current of 20 μA was selected for the concentration of the leading electrolyte used in our analyses, which was applied in previous experiments.

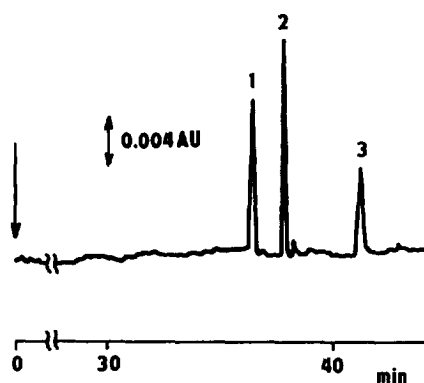Further, the influence of the CTAB concentration in the leading electrolyte on the peak width was

studied. Fig. 8 presents the dependence of length-based peak variance σ^2 of 3 pI markers on the CTAB concentration in logarithmic coordinates. The examined CTAB concentrations ranged from 0.05 mmol l^{-1} to 0.5 mmol l^{-1} (for other conditions see Fig. 7). Because of the pH gradient, the electro-osmotic flow changed along the capillary and thus the optimum CTAB concentration differed slightly for individual pI markers. In most of the experiments the concentration used was 0.15 mmol l^{-1}.

Further, for pI marker 15 the theoretically calculated σ value was compared with the observed σ value.

The observed σ value of 0.11 mm was determined from the linear velocity of the zone, 2.5 mm min^{-1}, measured in the transparent fused-silica capillary (4) and from the known value of the chart speed. The theoretical σ value was calculated according to the basic relationship published earlier [4,5]. The observed length of the pH gradient in the fused-silica capillary (4) was 10.5 mm between pI markers 19 and 3. The estimated steepness of the pH gradient, d pH/dx, was 0.32 pH mm^{-1}. The field potential, E, was taken as 18 V mm^{-1}. Based on the titration curve and the fact that zones move electrophoretical-
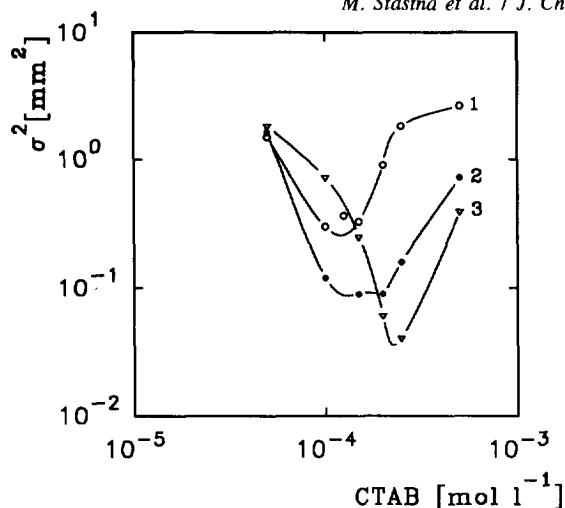
Fig. 8. Dependence of σ^2 on the concentration CTAB in leading electrolyte. σ^2=length-based peak variance (mm^2); $c=$ concentration CTAB (mol l^{-1}). (1) pI marker **19**, (2) pI marker **15**, (3) pI marker **3**. Other conditions as in Fig. 7.

Fig. 9. CDE of mixture of pI markers and myoglobin monitored at 280 nm. (1) pI marker **19** (0.32 mmol l^{-1}), (2) myoglobin (0.17 mmol l^{-1}), (3) pI marker **3** (0.04 mmol l^{-1}). Conditions: leading electrolyte, 10 mmol l^{-1} succinic acid and 7 mmol l^{-1} AMP, 0.15 mmol l^{-1} CTAB, 0.06% (w/v) HPMC; terminating electrolyte, 10 mmol l^{-1} AMP; background: 1.4% Ampholine pH 3.5–10.0; sample volume, 300 nl; background volume, 500 nl; I=10 μA; λ=280 nm; Spellman power supply.

ly, the slope $\mathrm{d}z/\mathrm{d}\,\mathrm{pH}$ was taken as -0.3 pH^{-1}. Then, σ for pI marker **15** was expected to be 0.12 mm. Despite the numerous approximations the agreement with the observed value is good. A further decrease of the peak width would need a decrease in the capillary cross-section and detection cell volume. Such improvements would also enable a decrease in separation time. Nevertheless, the separation performance obtained here was comparable to that achieved with an apparatus using a capillary of constant cross-section and a substantially higher potential; e.g., a similar separation of pI markers was obtained with a total capillary length of 58 cm or 90 cm and a constant total voltage of 20 kV [27]. In the referred paper a capillary with 75 μm I.D. allowed a complete analysis within 20 to 35 min.

Fig. 9 shows the CDE of a mixture of myoglobin and the two pI markers **19** and **3** having the pI values below and above the isoelectric point of myoglobin. At an applied current of 20 μA and the concentration of the leading electrolyte used in the previous experiments a precipitate of myoglobin appeared, which resulted in numerous interfering peaks in the electropherogram. The reason for this effect was the heat production in the capillary. However, conditions could be found under which these disturbances were eliminated. The leading electrolyte was diluted and
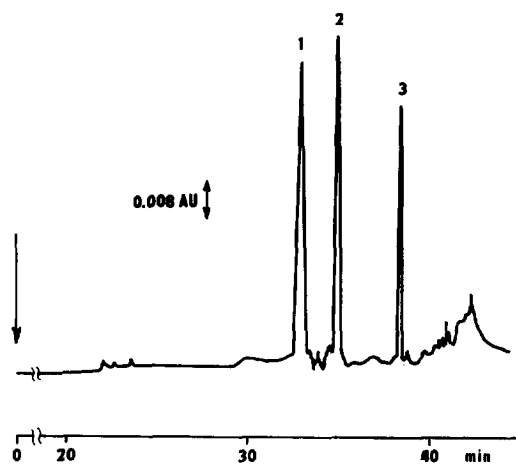
the current was decreased to such a value that the time of the analysis and the voltage profile were similar to those of previous experiments. In addition to the experiments performed at a the wavelength of 420 nm, analyses at wavelengths of 254 nm and 280 nm were examined. Fig. 9 shows an example of an experiment performed at 280 nm.

4. Conclusions

The automated instrument was designed to perform capillary displacement electrophoresis in short closed capillaries of nonuniform cross-section with a total volume of a few microliters. The device allowed unattended electrolyte renewal and injection of both the sample and spacers. The separation compartment made from organic glass, i.e. the tapered channel coupled to the fused-silica capillary, allowed both a reduction in the total voltage needed and on-column optical detection. Optimization of the

geometry of the separation compartment is in progress.

References

[1] P. Boček, M. Deml, P. Gebauer and V. Dolník, Analytical Isotachophoresis, VCH Verlagsgesellschaft, Weinheim, 1988.

[2] V. Kašička and Z. Prusík, J. Chromatogr., 569 (1991) 123.

[3] S. Hjertén and M. Kiessling-Johansson, J. Chromatogr., 550 (1991) 811.

[4] J.C. Giddings and K. Dahlgren, Sep. Sci., 6 (1971) 345.

[5] H. Svensson, Acta Chim. Scand., 15 (1961) 325.

[6] K. Šlais, J. Microcol. Sep., 5 (1993) 469.

[7] K. Šlais, J. Chromatogr. A, 679 (1994) 335.

[8] T. Izumi, T. Nagahori and T. Okuyama, J. High Resolut. Chromatogr., 14 (1991) 351.

[9] W. Thormann, J. Chromatogr., 334 (1985) 83.

[10] M.A. Firestone and W. Thormann, J. Chromatogr., 436 (1988) 309.

[11] T. Manabe, H. Yamamoto and T. Okueyama, Electrophoresis, 10 (1989) 172.

[12] Th.P.E.M. Verheggen, A.C. Schoots and F.M. Everaerts, J. Chromatogr., 503 (1990) 245.

[13] Th.P.E.M. Verheggen and F.M. Everaerts, J. Chromatogr., 638 (1993) 147.

[14] K. Šlais, Electrophoresis, 16 (1995) 2060.

[15] K. Šlais, J. Microcol. Sep., 7 (1995), 127.

[16] A.J.P. Martin and F.M. Everaerts, Anal. Chim. Acta, 38 (1967) 233.

[17] J. Pawliszyn and J. Wu, J. Microcol. Sep., 5 (1993) 397.

[18] K. Šlais, J. Chromatogr. A, 684 (1994) 149.

[19] P. Boček, M. Deml and J. Janák, J. Chromatogr., 106 (1975) 283.

[20] W. Thormann, A. Tsai, J.P. Michaud, R.A. Mosher and M. Bier, J. Chromatogr., 389 (1987) 75.

[21] A. Manz, D.J. Harrison, E.M.J. Verpoorte, J.C. Fettinger, A. Paulus, H. Lüdi and H.M. Widmer, J. Chromatogr., 593 (1992) 253.

[22] S.C. Jacobson, R. Hergenroder, L.B. Koutný and J.M. Ramsey, Anal. Chem., 66 (1994) 1107.

[23] M. Krejčí, V. Kahle, J. Chromatogr., 392 (1987) 133.

[24] F. Foret, M. Deml, V. Kahle and P. Boček, Electrophoresis 7 (1986) 430.

[25] K. Šlais and Z. Friedl, J. Chromatogr. A, 661 (1994) 249.

[26] K. Šlais and Z. Friedl, J. Chromatogr. A, 695 (1995) 113.

[27] J. Caslavska, S. Molteni, J. Chmelík, K. Šlais, F. Matulík and W. Thormann, J. Chromatogr. A, 680 (1994) 549.

[28] J. Pospíchal, M. Deml and P. Boček, Chem. Rev., 89 (1989) 419.

[29] V.A. Palm (Editor), Tables of Rate and Equilibrium Constants of Heterolytic Organic reactions, Vol. 2/1, VINITI, Moscow, 1975, p.45.

[30] W.J. Fergusson and N.E. Good, Anal. Biochem., 104 (1980) 300.

[31] T. Hirokawa and Y. Kiso, J. Chromatogr., 260 (1983) 225.

[32] P. Doležel, V. Kahle and M. Krejčí, Fresenius J. Anal. Chem., 345 (1993) 762.

[33] P. Doležel, M. Krejčí and V. Kahle, J. Chromatogr. A, 675 (1994) 47.

[34] K. Šlais, J. Chromatogr. A, 730 (1996) 247.

[35] J.C. Sternberg, in J.C. Giddings and R.A. Keller (Editors), Advances in Chromatography, Vol. 2, Marcel Dekker, New York, 1966.